Periodic Nanohole Arrays with Enhanced Lasing and Spontaneous Emissions for Low-cost Plasmonic Devices

Bryson Krause,[1] Minh T. Pham,[2] Hoang Mai Luong,[2] Tho Duc Nguyen,[2] and Thang B. Hoang[1,]*

[1]Department of Physics and Material Science, University of Memphis, Memphis, TN 38152

[2]Department of Physics & Astronomy, University of Georgia, Athens, GA 30602

[*]Author to whom correspondence should be addressed. Electronic mail: *tbhoang@memphis.edu*

Keywords: Plasmonics, nanohole arrays, nanolasers, Purcell enhancement, shadowing lithography.

ABSTRACT

Periodic arrays of air nanoholes in thin metal films that support surface plasmon resonances can provide an alternative approach for boosting the light-matter interactions at the nanoscale. Nanohole arrays have garnered great interest in recent years for their use in biosensing, light emission enhancement and spectroscopy. Here, we employ a simple technique to fabricate nanohole arrays and examine their photonic applications including enhanced lasing and spontaneous emission of novel nanomaterials. In contrast to the complicated and most commonly used electron beam lithography technique, hexagonal arrays of nanoholes are fabricated by using a simple combination of shadowing nanosphere lithography technique and electron-beam deposition. Through spectral and temporal characterizations, it was shown that these arrays offer an enhancement in the lasing emission of an organic dye liquid gain medium with a quality factor above 150 as well as an accelerated decay rate for CdSe quantum dots. The simple fabrication of

nanohole arrays together with their excellent optical responses can therefore offer a great potential in the industrialization of plasmonic devices for use in various realms of emerging technologies such as gas sensing, biomedical imaging and ultrafast on-chip coherent light sources.

I. INTRODUCTION

Periodic lattices of plasmonic nanostructures have attracted a considerable amount of attention in research and industry as a powerful tool for ultra-sensitive detection and high spectral resolution at the nanoscale level.[1-2] Nanostructured plasmonic metasurfaces such as nanoparticle or nanohole arrays have been exploited for a wide range of applications including biosensing, light harvesting, photonic and optofluidic devices.[3-10] Having been studied extensively over the last two decades, the attributes of many types and configurations of nanostructured arrays are thoroughly documented.[11-13] Therefore, there are many well-understood methods of fabrication which yield a variety of nanoarrays.[14-17] The ideal nanoarray involves a fabrication process that is simple, cheap and precise, though many of the nanoarray fabrication techniques used in practice are cumbersome and expensive.[18-19] Periodic arrays of plasmonic nanostructures are shown to exhibit strong tunable surface lattice plasmon resonances, which offer an excellent opportunity to engineer the light-matter interactions for useful applications in photonics and optoelectronics.[20] In contrast to localized surface plasmon offered by individual structures, periodic plasmonic arrays have the practical ability to strongly confine light via surface lattice plasmons, thus offering a way forward with controlling the light-matter interaction at an extended length scale of many lattice constants.[21-22] Previously, the use of liquid gain media in nanocavity arrays has been demonstrated to achieve a dynamically tunable lasing response, for instance, by using periodic arrays of nanoparticles.[23] Periodic nanohole arrays (PNAs), on the other hand, have either limited or unexplored

functionality when it comes to enhancing light emission such as lasing or photoluminescence. Though nanohole arrays are gaining traction for their use in open cavity systems, previous studies have scarcely demonstrated lasing action only in a low temperature environment by using metal hole arrays with a semiconductor gain medium.[24]

In this paper, the low-cost shadowing nanosphere lithography technique is employed for fabricating PNAs onto a glass substrate. Previously, the more conventional direct-write electron beam lithography (EBL) technique has been used commonly to fabricate periodic nanostructured arrays, including PNAs. However, EBL is an expensive technique as it requires cumbersome equipment, several complicated steps and a significant amount of time to execute. Such a technique poses a challenge in fabricating large-area arrays at low production costs. Another well-developed technique, namely PEEL (Photolithography, E-beam deposition, Etching, and Lift-off), can also offer high-quality, large-area arrays of plasmonic nanostructures.[22] Alternatively, large surface areas of PNAs can be rapidly fabricated by using a simple combination of shadowing nanosphere lithography technique and electron beam deposition. In contrast to the conventional lithography techniques, large surface area of PNAs can be rapidly fabricated by using a simple combination of shadowing nanosphere lithography technique and electron-beam deposition. By using a liquid gain fluorescent dye medium, PNA is demonstrated to induce an efficient lasing emission at room temperature. Furthermore, because of the high photonic density of states provided by an PNA, it is possible to increase the spontaneous emission rate of coupled quantum systems at particular wavelengths by tuning the PNA's plasmon resonance.[25] As a result, an accelerated decay rate of colloidal CdSe quantum dots (QDs) that are integrated with NPAs is demonstrated in this work. The design parameter that most influences an PNA plasmonic properties is the lattice constant of the array, which can be tailored through the shadowing

nanosphere lithography technique by controlling the size of colloidal nanospheres (or beads). Thus, the fabricated PNAs and their optical studies imply a potential flexible optical platform for applications in optoelectronics such as gas sensing,[26-28] biosensor and biomedical imaging[29-30] and optical engineering.[31-32]

II. METHODS

A. Nanohole array fabrication

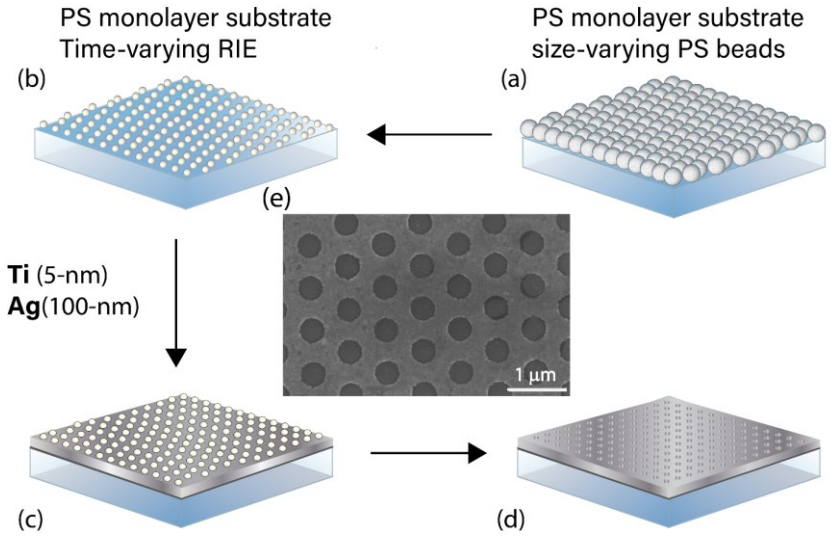

Figure 1. Nanohole array fabrication steps. (a) PS beads are deposited in a single layer onto a glass substrate. (b) PS beads are then subjected to RIE to decrease bead size, thus reducing the diameter of nanoholes. (c) 5-nm Ti and 100-nm Ag are deposited onto the PS/glass configuration. (d) The PS layer is then lifted from the assembly leaving a periodic hexagonal nanohole array. (e) SEM image of a nanohole array.

The fabrication of nanohole arrays used in this study begins with the deposition of a colloidal polystyrene (PS) nanosphere monolayer on a glass substrate through the air-water interface method, as described previously.[33] To summarize this method, the PS beads are first dissolved in a solution of water and ethanol, which is dropped slowly in small increments onto a glass petri dish containing a small amount of water. The surface area of the PNA, which is typically a few centimeters large in this present study, is determined by the size of the glass substrate. After some

time, the PS beads form a hexagonally close packed monolayer on the water-air interface, and a Teflon ring is placed around the surface to protect the monolayer from adhesion to the side of the petri dish. The water level is then raised, and a glass substrate is carefully slid beneath the PS monolayer film. The water then gets pumped out, and the PS monolayer film is lowered onto the glass substrate. Once the monolayer is lowered completely, the PS beads are subjected to reactive ion etching (RIE), effectively decreasing the bead size. After RIE, a 5-nm layer of Ti followed by a 100-nm Ag layer is deposited via the electron-beam evaporation onto the glass/PS array at the base pressure of 10^{-6} mbar. The Ti layer acts as a bonding agent between the glass substrate and the Ag layer. After layer deposition, the PS beads are stripped away from the assembly with Scotch tape, leaving behind a periodic hexagonal nanohole array in Ag. In this configuration, Ag coating was chosen over Au for its superior surface plasmon resonance properties, in contrast to the high loss in Au at optical frequencies. An alternative approach could implement Au or an Au/Ag hybrid coating instead of Ag to improve the degradation lifetime of the PNA, though such a construction may have weaker plasmonic responses than those offered by Ag-coated PNAs.[34] The controllable parameters in this process (Fig. 1 (a) - (d)) are the lattice spacing and nanohole size, which can be adjusted through the size of PS beads and RIE exposure time, respectively. The nanohole array samples presented here were fabricated by using two different sets of inter-particle spacing of 500 nm and 750 nm, by using different respective RIE times which resulted in different hole radii as we will present below. Figure 1(e) shows the scanning electron microscope (SEM) image of one of PNAs samples used for this work.

B. Sample characterization

In order to determine their resonant modes, each nanoarray was mounted onto a controllable turntable, and an angle-dependent transmission scan was taken for 45 degrees about normal

incidence. Figure 2(a) shows the peak resonances at normal incidence of arrays with lattice spacings of 500 nm and 750 nm resulting from two different particle sizes and RIE etching times of 300 s and 700 s, respectively. In this spectral range, the spectrum for 500-nm (750-nm) lattice spacing array contains well-defined transmission minima at 660 nm and at approximately 450-nm (700 nm) due to the (0, 1) Wood - Rayleigh anomaly modes, which are results of the surface plasmon waves at the metal/glass and metal/air interface, respectively. The observation of these transmission minima is consistent with the plasmonic-grating theory,[12, 35] and also in excellent agreement with our recent studies of a similar structure.[27, 36-37] In this situation the light that couples to these resonant modes is pointing in the direction perpendicular to the sample surface. This is very important, because the photons emitted by an embedded emissive nanomaterial will be guided by the directional resonance. At the transmission minimum (at ~ 660 nm for the Ag/glass mode or ~ 700 nm for the Ag/air mode) the full-width-at-half-maximum (FWHM) of these transmission curves were determined to be around 40-nm which results in an approximate quality factor of 16.

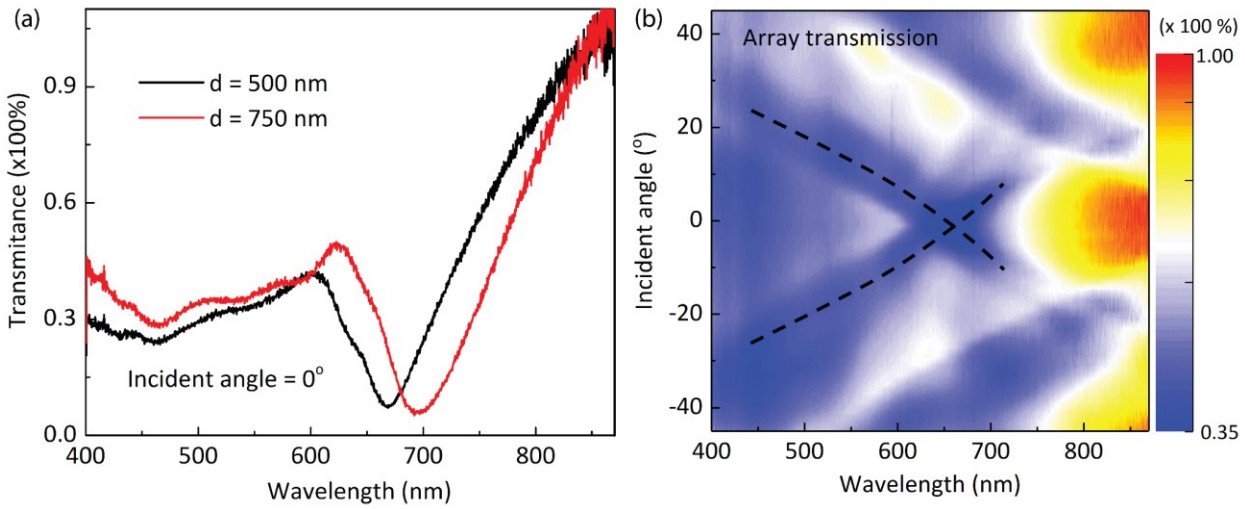

Figure 2. Optical characterizations of PNAs. (a) Transmission curves of PNAs for two different lattice sizes (500 and 750 nm) at the normal incident angle. (b) Angle-resolved transmission of a 500 nm-lattice PNA. Dashed lines indicate lattice plasmon resonances that follow the (0, ±1) Wood – Rayleigh modes.

Figure 2(b) shows a false-color image which was constructed by transmission spectra collected as a function of the incident angles of a 500-nm lattice array resulting from a RIE etching time of 300 s. The dashed curves indicate the (0, ±1) Wood - Rayleigh anomaly metal/glass mode position as a function of the incident angle. This observation is similar to the resonant modes that were observed by several previous reports.[38-41] In the following sections, we will be interested in this particular resonant mode, and the resonant wavelength at the normal incident angle will be used as a reference for the selection of appropriate fluorescent emitters.

C. Active materials integration and optical measurements

In order to probe the lasing enhancement behavior of the PNAs, several different configurations of active medium on glass slide and on nanoarray were prepared. To stimulate lasing, an organic fluorescent DCM dye [*4-(Dicyanomethylene)-2-methyl-6-(4-dimethylaminostyryl)-4H-pyran*] suspended in DMSO [*Dimethyl Sulfoxide*] was utilized as the active medium. The spectrum of DCM dye showed a resonant emission at around 663-nm, which nearly overlaps with the transmission minima at ~ 660-nm of the PNA (Figure 2(a), black curve). A range of concentrations of dye in DMSO was mixed in a vortexer and sonicated for 5 minutes, and 15 μL of each concentration was transferred with a pipette onto separate 1 cm square pieces of either slide glass or PNA to be used as a liquid gain medium for lasing. In an ideal configuration, the dye molecules would rest in the nanoholes. However, as this was not feasible with the methods used here, the dye molecules are assumed to have been mostly suspended above the nanoholes in the liquid medium. Spontaneous emission enhancement by the PNAs can also be demonstrated by observing the shortened decay time of QDs integrated into the nanoarrays. Several 1 cm^2 pieces of the 500-nm lattice, 150-nm radius hole PNA were covered with a diffuse concentration (0.01mg/mL) of CdSe QDs (Sigma Aldrich) suspended in toluene. The sample was spin-coated for 30 seconds at

1500 revolutions per minute. This configuration was washed clean with deionized water and flushed with clean nitrogen gas. Spectral analysis of the emission of the CdSe QDs confirmed the manufacturer's specified peak emission value of 655-nm, which is close to the PNA resonance at around 660-nm.

All optical measurements were taken at standard atmospheric pressure and at ambient temperature. Photoluminescence (PL) signals were captured with a CCD (charge-coupled device) camera and analyzed with a Horiba iHR550 spectrometer. For the decay time measurements of the quantum dots, a time-correlated single photon counting setup was used. An ultrafast Coherent laser at 475-nm (80MHz, 150fs) was used to excite the QDs through a 10X objective lens. The PL emission from the QDs was collected by the same objective lens and sent through the spectrometer for either spectral analysis or through a side exit to be guided into a fast-timing avalanche photodiode for temporal analysis. The signals collected by the photodiode were analyzed by a single photon counting module (PicoQuant PicoHarp 300). For the lasing experiment, DCM dye was excited by another Coherent laser at 515-nm (2 kHz, 2 ns pulse width) by using a 5x objective lens at a normal incident angle. The PL emission from the dye was collected by the same lens and then dispersed and analyzed by the spectrometer and CCD camera. It is also important to note that for the objective lenses used in our experiments, the excitation and collection spot size was approximately 100 μm in diameter, which covered an area of many lattice periods (Figs. 3(a) and 4(a)).

III. RESULTS AND DISCUSSION

In this section, we demonstrate the lasing action as well as enhanced spontaneous emission of quantum emitters by integrating them with the PNAs. Nanohole arrays with surface lattice plasmon resonances at around 665-nm were used. Because of this, organic DCM dye and colloidal CdSe QDs, which have a similar emission wavelength, were chosen as active materials. It is worth noting

that several similar experiments have previously demonstrated such applications of different nanoparticle arrays; our current purpose is to show that with an alternative simple fabrication technique, we can obtain similar results for potential useful applications in nanophotonics and optoelectronics at a lower cost and large-scale production.[23, 42]

A. Lasing enhancement

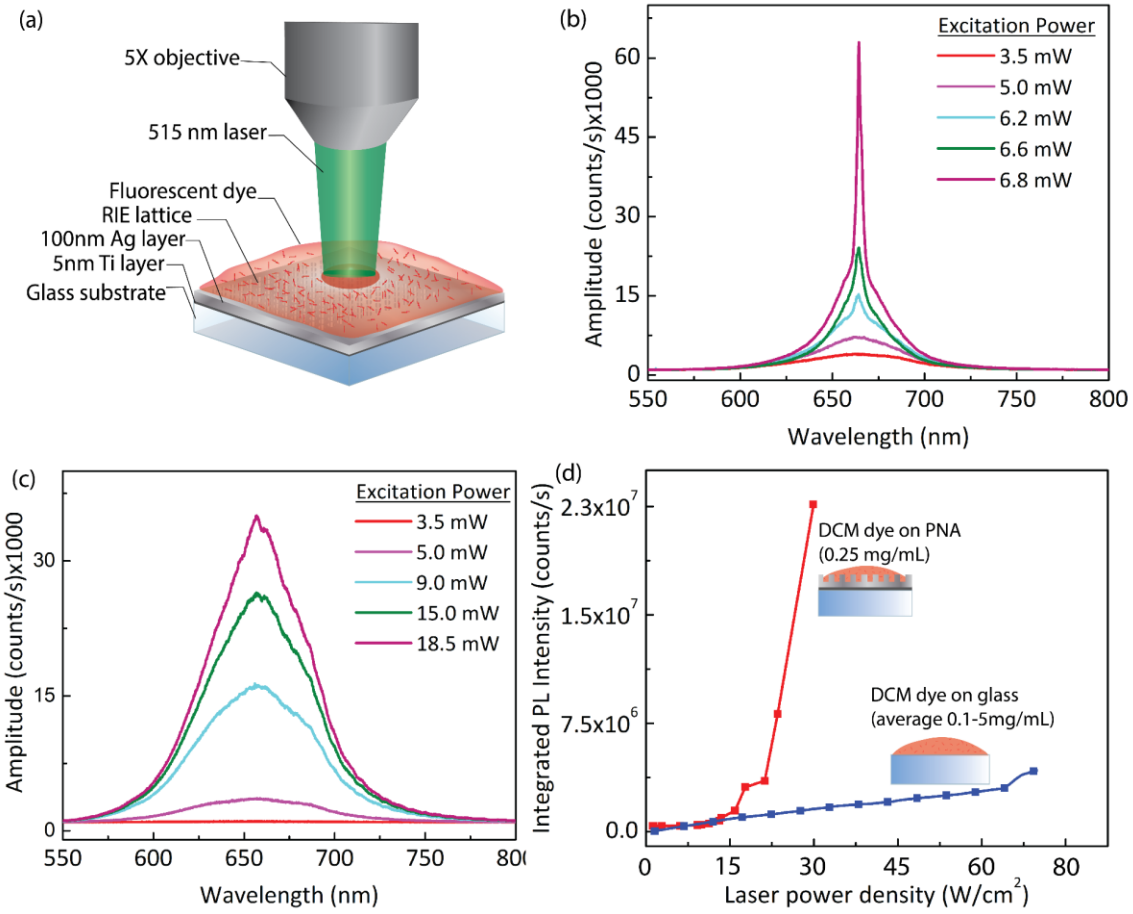

Figure 3. Enhanced lasing emission by PNAs. (a) Experimental setup consisting of a 2 kHz at 515-nm and 2 ns-pulse laser transmitted through a 5x objective onto a DCM-dye drop placed onto a 300-nm diameter nanohole array with a 500-nm lattice spacing. Power dependent PL spectra of 0.5 mg/mL dye on (b) nanoarray and (c) on glass. (d) Comparison between the integrated PL peak intensities of 0.25 mg/mL DCM dye on nanohole array and the average peak intensity of DCM dye concentrations on glass, ranging from 0.1 to 5 mg/mL. Square dots are data points and solid lines between dots are guides to the eye.

We first attempt to demonstrate potential applications of nanohole arrays by taking advantage of the surface lattice plasmon resonance to enhance lasing action of embedded organic DCM dye. This creates opportunities for developing plasmonic chips with integrated directional, efficient coherent light sources.

To investigate the lasing enhancement offered by the PNAs, the PL spectra were recorded for both DCM dye-covered glass and dye-covered 500-nm lattice (150-nm hole radius) at equal intervals starting at a power density of 11.3 $\frac{W}{cm^2}$ (or at 3.5 mW incident power) until CCD reading saturation, which occurred at around 59.7$\frac{W}{cm^2}$ for dye on glass, or until lasing was achieved for dye in PNA. Figures 3 (b) and (c) show the PL spectra of the DCM dye under various laser excitation power densities for a dye concentration of 0.5 mg/mL for both cases. It is also observed that the dye-covered nanoarray showed a more prominent lasing response at a lower excitation power than the dye/glass for multiple concentrations of dye. This lasing response began at a threshold of about 18.9$\frac{W}{cm^2}$, for dye on nanoarray, as indicated in the nonlinearity in the integrated peak intensity plot shown in Fig. 3(d), which shows the compared PL responses between nanoarray and glass with DCM dye. At a power density of 22.0 $\frac{W}{cm^2}$, a plasmonic supported lasing mode was fully evident in the nanohole array with a FWHM of 4.2-nm and a corresponding quality $Q = \frac{\lambda}{\Delta\lambda}$ greater than 150 (Fig. 3 (b), which is comparable with values presented in other studies using fluorescent emitters combined with comparable nanostructure arrays.[23, 43] For the same dye concentration on glass, even at high excitation densities the spectrum exhibits a broad PL band with a FWHM of 50-nm, indicating only spontaneous emission (Fig. 3(c)). It should be noted that the emission intensity of DCM dye on glass represented in Fig. 3 (d) is averaged for dye concentrations varying from 0.1 to 5mg/mL. For the larger concentration dyes on glass, lasing was evident at a high-

power density, however, for the same dye placed on PNA lasing occurred at a much lower power. At a concentration of 1mg/mL, for example, dye on glass exhibited lasing at a power density of about 69.0 $\frac{W}{cm^2}$ while the dye on PNA configuration began to lase at 19.7 $\frac{W}{cm^2}$ (result not plotted here), thus demonstrating a lasing threshold reduction factor of 3.5 for dye on PNA.

This lasing emission in PNAs has potential applications for on-chip coherent light sources, which can transcend the physical limitations imposed on conventional lasers by the optical diffraction limit.[44] Additionally, the use of organic dye as a liquid gain medium has been shown to be a promising method for providing a means of dynamic tunability in these type of plasmonic nanostructures.[21]

B. Enhanced spontaneous emission.

Novel nanomaterials, such as semiconductor quantum dots,[45-46] nanowires[47-48] or 2D dichalcogenides[49-50] offer properties and allow applications that do not exist in their macroscopic counterparts. However, current photonic devices based on these nanomaterials are limited by their intrinsic properties, including slow temporal emission (10-20 ns), low efficiency (10-15 %), and non-directional spatial emission. Integrating these nanomaterials with plasmonic nanocavities, which provide high photonic density of states, will significantly enhance their overall efficiency. As a result, such a device can significantly boost overall device efficiency to more than 50%[51-52] and operating frequency up to 90 GHz[52] yielding promise for photonic applications ranging from sensing and information processing to photovoltaics. Even though many plasmonic devices have previously demonstrated to offer significant enhanced optical properties such as PL intensity, spontaneous emission rate or surface enhanced Raman signal, our intent here is to demonstrate that PNAs could also provide an alternative path for enhancing these properties by integrating colloidal CdSe QDs with PNAs. While it is possible to achieve lasing emission with CdSe QDs, it

is exceedingly difficult especially at room temperature due to the Auger recombination process.[53] Therefore, even with the advantage of matching the emission of QDs with the plasmonic resonance of the PNA, the overall optical gain of the CdSe QDs is still very small (in comparison with that of the DCM dye, for example).

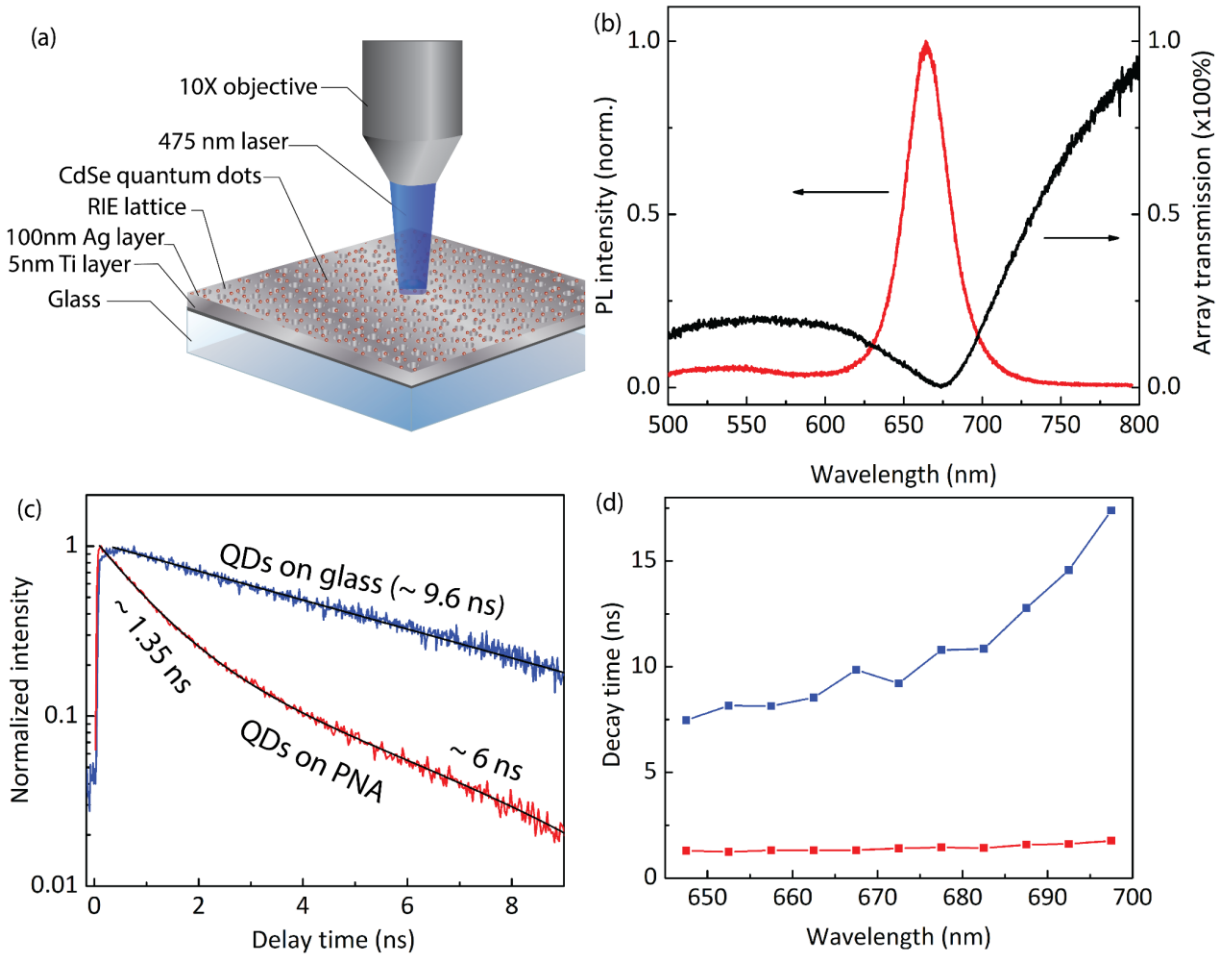

Figure 4. Enhanced spontaneous emission by PNAs. (a) Schematic of experimental setup for measuring CdSe QD-covered PNA. (b) Frequency matching between the PNA's transmission (black), PL emission of CdSe QDs on PNA (red). (c) Average measured decay curves of CdSe QDs on glass (black) and on a 500-nm lattice PNA (red). (d) Wavelength dependent decay times of QDs on glass and on the array (fast component). Square dots are data points while solid lines between dots are guides to the eye.

In our experiment, the PL and decay time measurements of a 500 nm-lattice, 150-nm radius hole PNA covered with CdSe QDs were taken and compared to that of the exact same CdSe QDs on a glass slide as control. The samples were excited with a power density of 3 $\frac{W}{cm^2}$ by a pulsed, frequency-doubled laser (Coherent Chameleon Ultra II, 80 MHz, 150 fs) tuned to 475-nm through a 10x objective (Fig. 4(a)). In order to take advantage of the lattice plasmon resonance of the PNA, the CdSe QDs are selected so their emission energy is exactly overlapping with the resonance of the array. Figure 4(b) shows the PL emission of the QDs, which is plotted together with a transmission curve of the nanohole array. The decay dynamics of the QD excitonic states were investigated by a time-correlated single photon counting module and decay curves were plotted as the coincident count vs. time for each sample, as shown in Fig. 4 (c). While the intrinsic decay time of QDs on a glass slide exhibits a single decay component, the QDs in the PNA appear to show a fast and a slow decay channel. From the fitting of the average of these plots spanning from the decay measured at 645 to 700-nm, a decay lifetime of 9.6 ns was determined for CdSe QDs on glass. For the fast and slow decay components of CdSe QDs on PNA, 1.35 ns and 6.0 ns were obtained at the peak transmission wavelength of the PNA. The faster decay time of the QDs in the array associated with an enhanced PL intensity therefore indicates an enhanced spontaneous emission rate of approximately 7. Several previous reports of the enhanced emission rate of quantum emitters integrated with nanoparticle arrays also show similar results.[54-55] Furthermore, the observed PL decay times in the array involved both QDs that coupled to the surface plasmon mode and QDs those did not couple to the lattice and the slow decay component observed from QDs in the array is related to the non-coupled QDs. It is important to note that the enhanced decay rate could also be related to the nonradiative quenching of the QDs when they in close proximity to a metal surface. In case of a strong nonradiative quenching the accelerated decay rate oftens

associated with a significant decrease of the PL emission intensity. In our expereiement we observed the PL emission intensity increased by a factor of 1.3 indicating that the Purcell enhancement effect is overcoming the nonradiative quenching effect. Figure 4(d) shows the decay times of QD on glass and PNA (the fast component) which were sampled at a 5-nm interval from 645-nm to 700-nm, following the bounds of each sample's PL curves. It is interesting to note that the QDs on the PNA exhibit a fast decay time across its emission spectrum, indicating the efficient coupling with the PNA's plasmon resonance.

The results of the lasing and spontaneous emission enhancement measurements described in this work point to several practical applications such as ultrafast light-emitting diodes, optical sensing or quantum information processing systems for this simple and inexpensive periodic PNA design. For example, it is possible to integrate a novel 2D nanomaterial such as WSe_2 or perovskite crystals having engineered defects with the PNAs to demonstrate a quantum plasmonic device for bright single photon sources.[56-57] It is also important to note that the described technique to fabricate PNAs can be applied to fabricate arrays of different shapes such as square–shaped holes if appropriate sized nanocubes are used as seed particles instead of spherical beads. Particularly, individual rectangle (or groove) shaped nanowaveguides can also be created, provided seed nanoparticles having specific shapes such as nanowires or nanorods, for further studies such as superradiance and quantum entanglement effects.[58-59] The control of a photonic material's spontaneous emission rate is key in the efficient generation of photons, and nanosize-based devices can be designed with this in mind.

IV. CONCLUSION

In summary, PNAs were designed and constructed by using a simple combination of shadowing nanosphere lithography technique and electron beam deposition. In contrast to the conventional electron beam lithography approach, the technique presented in this work is simple, cost-effective,

and more importantly, large area of high-quality metasurfaces can be rapidly fabricated. These arrays were demonstrated to have enhanced lasing capabilities when coupled with an organic dye in a liquid gain medium. Furthermore, the use of CdSe quantum dots on the arrays led to an enhanced spontaneous emission rate with a factor of approximately 7 times faster than that of QDs on a glass slide. Additionally, in contrast to prior demonstrations of highly deterministic emitter-cavity integration,[52, 60] the presented PNAs act as an open-cavity system which simplifies the design, avoiding the spatial mismatch between emitters and the optical modes of the cavity. These simple nanohole arrays can therefore further advance emerging technologies and propel in the industrialization of efficient plasmonic devices such as ppm-level gas detectors, biomedical imaging and point-of-care devices, stimulated amplification devices, and ultrafast on-chip coherent light sources.

Corresponding Author

Author to whom correspondence should be addressed. Electronic mail: *tbhoang@memphis.edu*

Author Contributions

T.H. conceived the idea of the research. B.K. performed the optical experiments, M. P. and H.L. performed the sample fabrication. T.H. and T.N. directed the research. All authors discussed the results and contributed to the manuscript.

Funding Sources

This work is supported by the National Science Foundation (NSF) (Grant # DMR-1709612). TH acknowledges the support from the FedEx Institute of Technology at the University of Memphis. UGA authors acknowledge the support from Thomas Jefferson Fund (Grant # RFACE0001080201).

Data Availability

The datasets generated during and/or analyzed during the current study are available from the corresponding author on reasonable request.

Competing Interests

The authors declare no conflict of interest.

REFERENCES

(1) Jiang, J.; Wang, X.; Li, S.; Ding, F.; Li, N.; Meng, S.; Li, R.; Qi, J.; Liu, Q.; Liu, G. L., Plasmonic nano-arrays for ultrasensitive bio-sensing. *Nanophotonics* **2018,** *7* (9), 1517-1531.

(2) Cervantes Tellez, G. A.; Hassan, S. a.; Tait, R. N.; Berini, P.; Gordon, R., Atomically flat symmetric elliptical nanohole arrays in a gold film for ultrasensitive refractive index sensing. *Lab on a Chip* **2013,** *13* (13), 2541-2546.

(3) Song, H. Y.; Wong, T. I.; Sadovoy, A.; Wu, L.; Bai, P.; Deng, J.; Guo, S.; Wang, Y.; Knoll, W.; Zhou, X., Imprinted gold 2D nanoarray for highly sensitive and convenient PSA detection via plasmon excited quantum dots. *Lab on a Chip* **2015,** *15* (1), 253-263.

(4) Psaltis, D.; Quake, S. R.; Yang, C., Developing optofluidic technology through the fusion of microfluidics and optics. *Nature* **2006,** *442* (7101), 381-386.

(5) Boriskina, S. V.; Ghasemi, H.; Chen, G., Plasmonic materials for energy: From physics to applications. *Materials Today* **2013,** *16* (10), 375-386.

(6) Anker, J. N.; Hall, W. P.; Lyandres, O.; Shah, N. C.; Zhao, J.; Van Duyne, R. P., Biosensing with plasmonic nanosensors. *Nature Materials* **2008,** *7* (6), 442-453.

(7) Butkus, J.; Edwards, A. P.; Quacquarelli, F. P.; Adawi, A. M., Light emission enhancement using randomly distributed plasmonic nanoparticle arrays. *Optical Materials* **2014,** *36* (9), 1502-1505.

(8) Escobedo, C.; Brolo, A. G.; Gordon, R.; Sinton, D., Optofluidic Concentration: Plasmonic Nanostructure as Concentrator and Sensor. *Nano Letters* **2012,** *12* (3), 1592-1596.

(9) Lee, M.; Kim, J. U.; Lee, K. J.; Ahn, S.; Shin, Y.-B.; Shin, J.; Park, C. B., Aluminum Nanoarrays for Plasmon-Enhanced Light Harvesting. *ACS Nano* **2015,** *9* (6), 6206-6213.

(10) Hoang Mai, L.; Minh Thien, P.; George Keefe, L.; Tho Duc, N. In *Plasmonic sensing of hydrogen in Pd nano-hole arrays*, Proc.SPIE, 2019.

(11) Wang, Y.; Ta, V. D.; Gao, Y.; He, T. C.; Chen, R.; Mutlugun, E.; Demir, H. V.; Sun, H. D., Stimulated Emission and Lasing from CdSe/CdS/ZnS Core-Multi-Shell Quantum Dots by Simultaneous Three-Photon Absorption. *Advanced Materials* **2014,** *26* (18), 2954-2961.

(12) Ebbesen, T. W.; Lezec, H. J.; Ghaemi, H. F.; Thio, T.; Wolff, P. A., Extraordinary optical transmission through sub-wavelength hole arrays. *Nature* **1998,** *391* (6668), 667-669.

(13) Abujetas, D. R.; Sánchez-Gil, J. A., Near-Field Excitation of Bound States in the Continuum in All-Dielectric Metasurfaces through a Coupled Electric/Magnetic Dipole Model. *Nanomaterials* **2021,** *11* (4).

(14) Hua, F.; Sun, Y.; Gaur, A.; Meitl, M. A.; Bilhaut, L.; Rotkina, L.; Wang, J.; Geil, P.; Shim, M.; Rogers, J. A.; Shim, A., Polymer Imprint Lithography with Molecular-Scale Resolution. *Nano Letters* **2004,** *4* (12), 2467-2471.

(15) Whitney, A. V.; Myers, B. D.; Van Duyne, R. P., Sub-100 nm Triangular Nanopores Fabricated with the Reactive Ion Etching Variant of Nanosphere Lithography and Angle-Resolved Nanosphere Lithography. *Nano Letters* **2004,** *4* (8), 1507-1511.

(16) Mirkin, C. A., The Power of the Pen: Development of Massively Parallel Dip-Pen Nanolithography. *ACS Nano* **2007,** *1* (2), 79-83.

(17) Liu, H.; Luo, Y.; Kong, W.; Liu, K.; Du, W.; Zhao, C.; Gao, P.; Zhao, Z.; Wang, C.; Pu, M.; Luo, X., Large area deep subwavelength interference lithography with a 35 nm half-period based on bulk plasmon polaritons. *Opt. Mater. Express* **2018,** *8* (2), 199-209.

(18) Broers, A. N.; Welland, M. E.; Gimzewski, J. K., Fabrication limits of electron beam lithography and of UV, X -ray and ion-beam lithographies. *Philosophical Transactions of the Royal Society of London. Series A: Physical and Engineering Sciences* **1995,** *353* (1703), 291-311.

(19) Song, J.-H.; Atay, T.; Shi, S.; Urabe, H.; Nurmikko, A. V., Large Enhancement of Fluorescence Efficiency from CdSe/ZnS Quantum Dots Induced by Resonant Coupling to Spatially Controlled Surface Plasmons. *Nano Letters* **2005,** *5* (8), 1557-1561.

(20) Anantharaman, S. B.; Jo, K.; Jariwala, D., Exciton–Photonics: From Fundamental Science to Applications. *ACS Nano* **2021,** *15* (8), 12628-12654.

(21) Ozbay, E., Plasmonics: Merging Photonics and Electronics at Nanoscale Dimensions. *Science* **2006,** *311* (5758), 189.

(22) Wang, W.; Ramezani, M.; Väkeväinen, A. I.; Törmä, P.; Rivas, J. G.; Odom, T. W., The rich photonic world of plasmonic nanoparticle arrays. *Materials Today* **2018,** *21* (3), 303-314.

(23) Yang, A.; Hoang, T. B.; Dridi, M.; Deeb, C.; Mikkelsen, M. H.; Schatz, G. C.; Odom, T. W., Real-time tunable lasing from plasmonic nanocavity arrays. *Nature Communications* **2015,** *6* (1), 6939.

(24) van Beijnum, F.; van Veldhoven, P. J.; Geluk, E. J.; de Dood, M. J. A.; 't Hooft, G. W.; van Exter, M. P., Surface Plasmon Lasing Observed in Metal Hole Arrays. *Physical Review Letters* **2013,** *110* (20), 206802.

(25) Fusella, M. A.; Saramak, R.; Bushati, R.; Menon, V. M.; Weaver, M. S.; Thompson, N. J.; Brown, J. J., Plasmonic enhancement of stability and brightness in organic light-emitting devices. *Nature* **2020,** *585* (7825), 379-382.

(26) Luong, H. M.; Pham, M. T.; Guin, T.; Madhogaria, R. P.; Phan, M.-H.; Larsen, G. K.; Nguyen, T. D., Sub-second and ppm-level optical sensing of hydrogen using templated control of nano-hydride geometry and composition. *Nature Communications* **2021,** *12* (1), 2414.

(27) Luong, H. M.; Pham, M. T.; Nguyen, T. D.; Zhao, Y., Enhanced Resonant Faraday Rotation in Multilayer Magnetoplasmonic Nanohole Arrays and Their Sensing Application. *The Journal of Physical Chemistry C* **2019,** *123* (46), 28377-28384.

(28) Pham, M. T.; Luong, H. M.; Pham, H. T.; Guin, T.; Zhao, Y.; Larsen, G. K.; Nguyen, T. D., Pd80Co20 Nanohole Arrays Coated with Poly(methyl methacrylate) for High-Speed Hydrogen Sensing with a Part-per-Billion Detection Limit. *ACS Applied Nano Materials* **2021,** *4* (4), 3664-3674.

(29) Prasad, A.; Choi, J.; Jia, Z.; Park, S.; Gartia, M. R., Nanohole array plasmonic biosensors: Emerging point-of-care applications. *Biosensors and Bioelectronics* **2019,** *130*, 185-203.

(30) Li, X.; Soler, M.; Özdemir, C. I.; Belushkin, A.; Yesilköy, F.; Altug, H., Plasmonic nanohole array biosensor for label-free and real-time analysis of live cell secretion. *Lab on a Chip* **2017,** *17* (13), 2208-2217.

(31) Huang, F. M.; Zheludev, N.; Chen, Y.; Javier Garcia de Abajo, F., Focusing of light by a nanohole array. *Applied Physics Letters* **2007,** *90* (9), 091119.

(32) Rodrigo, S. G., Amplification of stimulated light emission in arrays of nanoholes by plasmonic absorption-induced transparency. *Opt. Express* **2021,** *29* (19), 30715-30726.

(33) Ingram, W.; Larson, S.; Carlson, D.; Zhao, Y., Ag–Cu mixed phase plasmonic nanostructures fabricated by shadow nanosphere lithography and glancing angle co-deposition. *Nanotechnology* **2016,** *28* (1), 015301.

(34) Murray-Méthot, M.-P.; Ratel, M.; Masson, J.-F., Optical Properties of Au, Ag, and Bimetallic Au on Ag Nanohole Arrays. *The Journal of Physical Chemistry C* **2010,** *114* (18), 8268-8275.

(35) Martín-Moreno, L.; García-Vidal, F. J.; Lezec, H. J.; Pellerin, K. M.; Thio, T.; Pendry, J. B.; Ebbesen, T. W., Theory of Extraordinary Optical Transmission through Subwavelength Hole Arrays. *Physical Review Letters* **2001,** *86* (6), 1114-1117.

(36) Hessel, A.; Oliner, A. A., A New Theory of Wood's Anomalies on Optical Gratings. *Appl. Opt.* **1965,** *4* (10), 1275-1297.

(37) Luong, H. M.; Ai, B.; Zhao, Y.; Nguyen, T. D., Weak enhanced resonant Faraday rotation in pure cobalt plasmonic lattices: Thickness dependent Faraday rotation studies. *Journal of Magnetism and Magnetic Materials* **2018,** *468*, 79-84.

(38) Parsons, J.; Hendry, E.; Burrows, C. P.; Auguié, B.; Sambles, J. R.; Barnes, W. L., Localized surface-plasmon resonances in periodic nondiffracting metallic nanoparticle and nanohole arrays. *Physical Review B* **2009,** *79* (7), 073412.

(39) Monteiro, J. P.; Carneiro, L. B.; Rahman, M. M.; Brolo, A. G.; Santos, M. J. L.; Ferreira, J.; Girotto, E. M., Effect of periodicity on the performance of surface plasmon resonance sensors based on subwavelength nanohole arrays. *Sensors and Actuators B: Chemical* **2013,** *178*, 366-370.

(40) Wu, L.; Bai, P.; Zhou, X.; Li, E. P., Reflection and Transmission Modes in Nanohole-Array-Based Plasmonic Sensors. *IEEE Photonics Journal* **2012,** *4* (1), 26-33.

(41) Najiminaini, M.; Vasefi, F.; Kaminska, B.; Carson, J. J. L., Nano-hole array structure with improved surface plasmon energy matching characteristics. *Applied Physics Letters* **2012,** *100* (4), 043105.

(42) Naveed, H. B.; Popov, S.; Shafique, M., Model microcavity laser with CdSe/CdS quantum dots as lasing media. *Laser Physics* **2016,** *26* (2), 025004.

(43) Fernandez-Bravo, A.; Wang, D.; Barnard, E. S.; Teitelboim, A.; Tajon, C.; Guan, J.; Schatz, G. C.; Cohen, B. E.; Chan, E. M.; Schuck, P. J.; Odom, T. W., Ultralow-threshold, continuous-wave upconverting lasing from subwavelength plasmons. *Nature Materials* **2019,** *18* (11), 1172-1176.

(44) Hill, M. T.; Gather, M. C., Advances in small lasers. *Nature Photonics* **2014,** *8* (12), 908-918.

(45) Reithmaier, J. P.; Sęk, G.; Löffler, A.; Hofmann, C.; Kuhn, S.; Reitzenstein, S.; Keldysh, L. V.; Kulakovskii, V. D.; Reinecke, T. L.; Forchel, A., Strong coupling in a single quantum dot–semiconductor microcavity system. *Nature* **2004,** *432* (7014), 197-200.

(46) Redl, F. X.; Cho, K. S.; Murray, C. B.; O'Brien, S., Three-dimensional binary superlattices of magnetic nanocrystals and semiconductor quantum dots. *Nature* **2003,** *423* (6943), 968-971.

(47) Yan, R.; Gargas, D.; Yang, P., Nanowire photonics. *Nature Photonics* **2009,** *3* (10), 569-576.

(48) Guo, X.; Ying, Y.; Tong, L., Photonic Nanowires: From Subwavelength Waveguides to Optical Sensors. *Accounts of Chemical Research* **2014,** *47* (2), 656-666.

(49) Manzeli, S.; Ovchinnikov, D.; Pasquier, D.; Yazyev, O. V.; Kis, A., 2D transition metal dichalcogenides. *Nature Reviews Materials* **2017,** *2* (8), 17033.

(50) Choi, W.; Choudhary, N.; Han, G. H.; Park, J.; Akinwande, D.; Lee, Y. H., Recent development of two-dimensional transition metal dichalcogenides and their applications. *Materials Today* **2017,** *20* (3), 116-130.

(51) Schlehahn, A.; Thoma, A.; Munnelly, P.; Kamp, M.; Höfling, S.; Heindel, T.; Schneider, C.; Reitzenstein, S., An electrically driven cavity-enhanced source of indistinguishable photons with 61% overall efficiency. *APL Photonics* **2016,** *1* (1), 011301.

(52) Hoang, T. B.; Akselrod, G. M.; Mikkelsen, M. H., Ultrafast Room-Temperature Single Photon Emission from Quantum Dots Coupled to Plasmonic Nanocavities. *Nano Letters* **2016,** *16* (1), 270-275.

(53) Park, Y.-S.; Bae, W. K.; Baker, T.; Lim, J.; Klimov, V. I., Effect of Auger Recombination on Lasing in Heterostructured Quantum Dots with Engineered Core/Shell Interfaces. *Nano Letters* **2015,** *15* (11), 7319-7328.

(54) Michieli, N.; Kalinic, B.; Scian, C.; Cesca, T.; Mattei, G., Emission Rate Modification and Quantum Efficiency Enhancement of Er3+ Emitters by Near-Field Coupling with Nanohole Arrays. *ACS Photonics* **2018,** *5* (6), 2189-2199.

(55) Brolo, A. G.; Kwok, S. C.; Cooper, M. D.; Moffitt, M. G.; Wang, C. W.; Gordon, R.; Riordon, J.; Kavanagh, K. L., Surface Plasmon−Quantum Dot Coupling from Arrays of Nanoholes. *The Journal of Physical Chemistry B* **2006,** *110* (16), 8307-8313.

(56) He, Y.-M.; Clark, G.; Schaibley, J. R.; He, Y.; Chen, M.-C.; Wei, Y.-J.; Ding, X.; Zhang, Q.; Yao, W.; Xu, X.; Lu, C.-Y.; Pan, J.-W., Single quantum emitters in monolayer semiconductors. *Nature Nanotechnology* **2015,** *10* (6), 497-502.

(57) Wu, S.; Buckley, S.; Jones, A. M.; Ross, J. S.; Ghimire, N. J.; Yan, J.; Mandrus, D. G.; Yao, W.; Hatami, F.; Vučković, J.; Majumdar, A.; Xu, X., Control of two-dimensional excitonic light emission via photonic crystal. *2D Materials* **2014,** *1* (1), 011001.

(58) Li, Y.; Nemilentsau, A.; Argyropoulos, C., Resonance energy transfer and quantum entanglement mediated by epsilon-near-zero and other plasmonic waveguide systems. *Nanoscale* **2019,** *11* (31), 14635-14647.

(59) Issah, I.; Caglayan, H., Qubit–qubit entanglement mediated by epsilon-near-zero waveguide reservoirs. *Applied Physics Letters* **2021,** *119* (22), 221103.

(60) Hoang, T. B.; Akselrod, G. M.; Argyropoulos, C.; Huang, J.; Smith, D. R.; Mikkelsen, M. H., Ultrafast spontaneous emission source using plasmonic nanoantennas. *Nature Communications* **2015,** *6* (1), 7788.

Table of Contents (TOC) graphic